The Tapered Slot Antenna—A New Integrated Element for Millimeter-Wave Applications

K. SIGFRID YNGVESSON, MEMBER, IEEE, T. L. KORZENIOWSKI, MEMBER, IEEE, YOUNG-SIK KIM, ERIK L. KOLLBERG, SENIOR MEMBER, IEEE, AND JOAKIM F. JOHANSSON

(Invited Paper)

Abstract—**Tapered slot antennas (TSA's) have a number of potential applications as single elements and focal plane arrays. TSA's can be fabricated with photolithographic techniques and integrated in either hybrid or MMIC circuits with receiver or transmitter components. They offer considerably narrower beams than other integrated antenna elements and have high aperture efficiency and packing density as array elements. Typical applications which have been demonstrated or are under development are reviewed.**

I. INTRODUCTION

IN MANY applications of millimeter-wave integrated circuits, power is either radiated or received by an antenna element. Ideally, one would then prefer to be able to integrate the antenna and the rest of the circuit on a single substrate or fabricate both parts of the subsystem as integrated components which can be joined easily. Antenna elements or arrays which radiate a broadside beam may use microstrip patches, dipoles, or slots. Antennas of this type integrated with different types of circuits have been studied extensively and implemented successfully into subsystems [1]. This paper describes an alternative integrated antenna element which has received attention recently—the (end-fire) tapered slot antenna (TSA) element. A typical TSA consists of a tapered slot which has been etched in the metallization on a dielectric substrate. Fig. 1 shows three TSA elements with different shapes of the taper—the "Vivaldi" (exponential taper), the LTSA (linear taper), and the CWSA (the primary radiating portion of the slot has constant width). TSA elements radiate along the long direction of the substrate and can also be easily combined into arrays (see Fig. 2). Whereas arrays of microstrip patches typically have all elements located on a single substrate, two-dimensional arrays of TSA's require a number of substrates equal to the linear dimension of the array. TSA single elements and arrays have some important advantages which make them potentially very well suited to a number of applications:

- Much narrower beam widths (down to 15° −3 dB beam width, and 30° −10 dB beam width) and higher antenna element gain can be achieved. This makes it feasible to illuminate reflector antennas and lenses directly with low spillover losses.
- The radiating portion of the TSA is well separated from the integrated circuit which follows it, and there is ample space for the latter. The circuit connection to the TSA can be accomplished in several ways, such as a transition to finline or implementing the circuit in slotline, as will be discussed later.
- The transverse spacing between TSA array elements can be made very small, even when the radiated element pattern has a narrow beam width. This feature is advantageous in many applications.

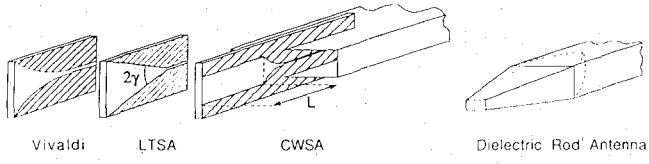

Fig. 1. The three different types of end-fire tapered slot antennas considered in this paper. A dielectric rod antenna is shown for comparison.

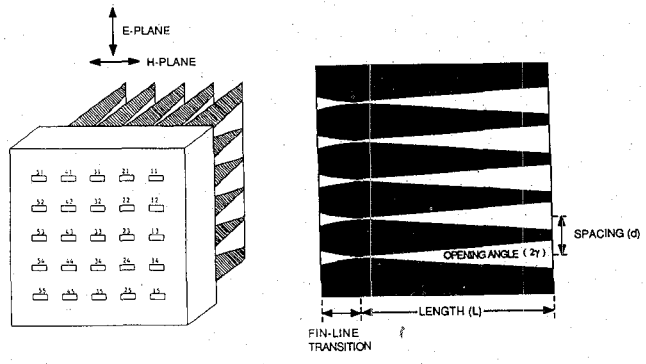

Fig. 2. A typical LTSA array (5×5 elements) with a finline to waveguide feeding block. The pattern etched on one of the substrates is shown to the right.

Manuscript received January 25, 1988; revised July 18, 1988. This work was supported by the NASA Langley Research Center under Contract NAS1-18310, by the Aerojet Electrosystems Corporation, Azuza, CA, by Frequency Sources, Lowell, MA, and by the Swedish Board for Technical Development.

K. S. Yngvesson and Y. S. Kim are with the Department of Electrical and Computer Engineering, University of Massachusetts, Amherst, MA 01003.

T. L. Korzeniowski is with the Missile Systems Division, Raytheon Company, Bedford, MA 01730.

E. L. Kollberg and J. F. Johansson are with the Department of Radio and Space Science, Chalmers University of Technology, Gothenburg, Sweden.

IEEE Log Number 8824990.

- The band width is much wider than for typical broadside antenna elements (excepting the log-periodic and spiral types), in some cases more than two octaves [2].

Single-element TSA's can be applied as feeds for reflector or lens antennas, and we will describe examples of SIS mixers integrated with TSA's. Alternatively, one may utilize the fairly high gain of TSA single elements (up to 17 dB) directly. Such antennas are very inexpensive to fabricate and could be useful as low-cost integrated antenna/receiver/transmitter units.

Arrays of TSA's have a number of potential applications. For example, high-resolution millimeter-wave imaging has been demonstrated with prototype TSA/reflector systems. TSA arrays could provide lightweight alternatives for focal-plane applications in satellite communication antennas involving beam shaping and beam switching. We also present data in this paper regarding phased arrays of TSA's.

This paper reviews information regarding TSA's in terms of their properties as radiating elements as well as circuit elements, information which so far has not been available in a single paper. Some very recent research results have also been incorporated to make the review up to date.

II. Review of Characteristics of TSA Single Elements

A. Beam Width, Directivity, and Gain of TSA Single Elements

Tapered slot antennas belong to the class of traveling-wave antennas of the "surface-wave" type; i.e., they utilize a traveling wave propagating along the antenna structure with a phase velocity $v_{ph} < c$. Another example of a surface-wave antenna is the dielectric rod antenna [3], also shown in Fig. 1. Despite the completely planar geometry of the TSA, it can produce symmetric radiation patterns in the planes parallel to the substrate (the E plane) and perpendicular to the substrate (the H plane). The review by Zucker [4] in Jasik's *Antenna Engineering Handbook* is especially useful in establishing the expected behavior with respect to beam width and directivity for traveling-wave antennas. The beam width narrows, and the directivity increases, as the length (L) of the antenna is increased. For a traveling-wave antenna with a constant phase velocity, there is an optimum phase velocity ratio $p = c/v_{ph} = 1 + \lambda_0/2L$, which results in *maximum directivity*, Zucker's "high-gain" case. This is equivalent to saying that there should be a total phase increase of 180° due to dielectric slowing for the wave traveling along the antenna structure. For a larger total phase shift than this, the beam moves into invisible space, and a null develops on the axis, rendering the antenna useless. In most TSA's the phase velocity is not constant along the antenna, and the situation is similar to that of a tapered dielectric rod antenna, classified by Zucker as the "low-sidelobe" case, with somewhat lower directivity than the high-gain case. The phase velocity along a TSA may be varied by changing the dielectric thickness, the dielectric constant, or the taper shape, so that beam widths are obtained which are in the range covered by these two standard cases of traveling-wave antennas. The case of air dielectric ($p = 1$) also results in a useful antenna [5], but with a somewhat wider beam width. Another general constraint for TSA's is that the slot width should reach at least one half wavelength for effective radiation to occur.

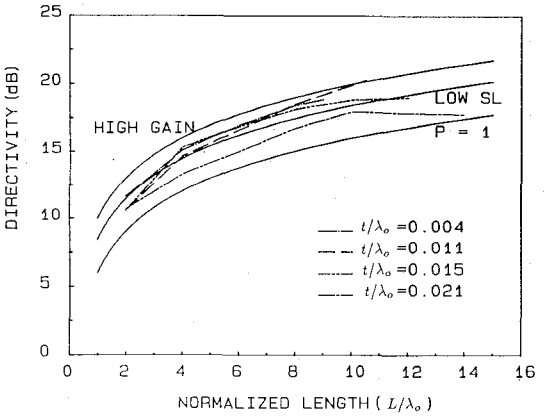

Fig. 3. Directivity estimated from (2) using measured patterns for LTSA's on substrates of four different thicknesses (t) plotted versus normalized length (L/λ_0). Three curves representing standard traveling wave antennas are also shown.

The directivity and beam width for the standard cases are usually plotted versus antenna length normalized to the free-space wavelength. Directivities and beam widths for LTSA's on Kapton ($\epsilon_r = 3.5$) with different substrate thicknesses are shown in Figs. 3 and 4, also including the prediction for the air dielectric case ($p = 1$). Further data are given in [6]–[8]. With the typical dielectric thickness used, the beam widths fall between the low-side-lobe and high-gain cases. The directivity of TSA's follows the length dependence of the standard cases but with somewhat lower values, generally, as discussed in detail below. The beam widths, and beam shapes, also agree quite well with theoretical calculations, provided that the width of the substrate is at least six wavelengths [8]. These calculations assume a traveling wave along the tapered slot and use a calculated phase velocity, which has to be adjusted slightly to agree with experimental measurements on wide slots [8]. Further calculations are in progress for the more difficult case of narrower substrates [9]. Preliminary results indicate good agreement for LTSA's with air dielectric. An analytical theory exists for the infinitely wide air-dielectric (TEM) LTSA [5]. The H-plane beam width follows Zucker's curves for such TEM LTSA's, while the E-plane beam width narrows faster than this as the length is increased.

From the above studies, one can identify an approximate optimum range of about 0.005 to 0.03 for the effective dielectric thickness of the substrate normalized to the free-space wavelength λ_0, which is defined by

$$\frac{t_{\text{eff}}}{\lambda_0} = \left(\sqrt{\epsilon_r} - 1\right)\frac{t}{\lambda_0} \tag{1}$$

(t is the actual substrate thickness). For thinner substrates,

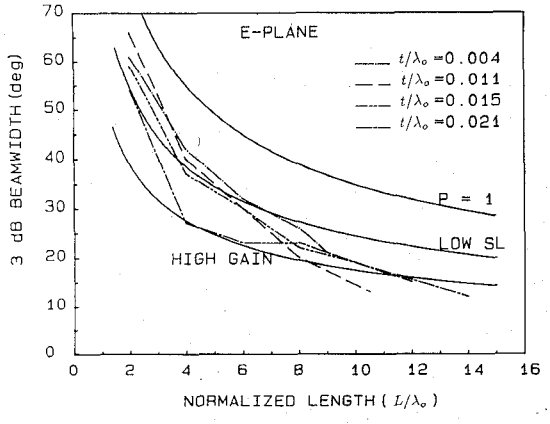

Fig. 4. 3 dB beam width versus normalized length for the same LTSA's as in Fig. 3. (a) *E* plane. (b) *H* plane.

the beam width will be wider, while for thicker substrates, the main beam will break up, as discussed earlier. It is therefore especially important to observe the upper limit to the thickness of the substrate, and we will return to this question below.

The standard method of finding the directivity for a feed antenna is to integrate the measured (copolarized) *E*- and *H*-plane patterns as follows:

$$D = \frac{4}{\int_0^{\pi} \left(|F_E(\theta)|^2 + |F_H(\theta)|^2 \right) \sin\theta \, d\theta}. \qquad (2)$$

The directivity calculated in this manner agrees well with Zucker's standard cases (see Fig. 3), which is expected since it reflects the behavior of the beam width and the fact that the side lobes are as low as for typical traveling-wave antennas. A measurement of the gain can be obtained for TSA's with a finline/waveguide transition by comparing the signal picked up by a waveguide detector from the TSA output with that of a standard gain horn, using the same detector. The measured value of the attenuation of the finline/waveguide transition (0.75 dB at 35 GHz) is added to the detected power from the TSA, so that the gain will be referred to the input of this transition. The gains measured in this way are generally lower by 2–4 dB than the directivities estimated as described above. We have found it necessary to integrate the radiation patterns for both copolarized and cross-polarized radiation, using data for the *E*, *H*, and *D* (diagonal) planes, in order to obtain better agreement between directivity (D) estimated from radiation patterns and the measured absolute gain (G). Estimated by this method, D is usually about 0.5–1 dB higher than G. The implications of these results are that 1) the radiation pattern has a more complicated symmetry than for typical feeds and 2) some power is "lost" to the cross-polarized pattern. We are presently studying methods for minimizing this cross-polarized power, and have very recently demonstrated substantially lower levels of cross-polarization losses.

We may define G/D as the radiation efficiency of the feed, and obtain typical values of about 80 percent. Maximum measured gain is about 16–17 dB for long elements.

B. Beam Shape, Effect of Different Taper Shapes

In general, the beam widths are narrowest for the CWSA shape, followed by the LTSA, and then the Vivaldi when compared on the same substrate with the same length and the same aperture size. As expected, the side lobes are highest for the CWSA, followed by the LTSA, and the Vivaldi. Further examples of radiation patterns are given in [10] and [11]. Typical LTSA's have opening angles (2γ) in the range 5–12°. The *E*-plane beam width narrows somewhat as 2γ is increased while the *H*-plane beam width is independent of this variable.

C. Impedance

The input impedance of an LTSA without a dielectric can be predicted by using conformal mapping [12]. Measured values for a "double" LTSA, as a function of opening angle of the taper, agree well with this theoretical prediction [6]. A typical LTSA with dielectric was found to have an input impedance of 80 Ω, independent of frequency over a 3:1 frequency range. Similar impedance values are also expected for other shapes, since the detailed shape of the feed region is unlikely to influence the impedance very much. The fact that the impedance varies so little is an advantage in applications of TSA's.

D. Effects of a Thick Dielectric

Fig. 5(a) illustrates the effects which occur if the effective dielectric thickness is too large. In this case, a Duroid 6010 substrate (dielectric constant = 10) with a thickness of 0.25 mm was used for an LTSA measured at 35 GHz. The normalized effective thickness is about 0.06 (compare (1)). One can regain a usable beam shape when using this substrate by eliminating the substrate in the tapered region, as shown in Fig. 5(b). The dielectric still has an effect at the edge of the taper; i.e., the beam width is considerably narrower than for the air-dielectric case. Similar techniques are expected to be useful in extending the use of TSA's to higher frequencies and higher dielectric constant substrates, such as silicon and GaAs.

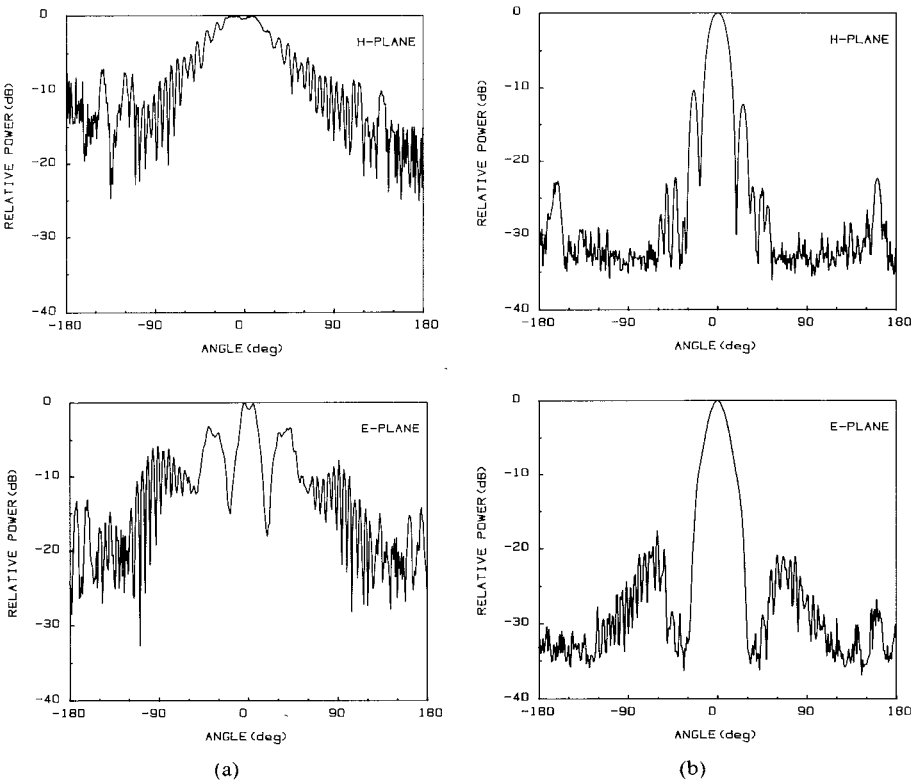

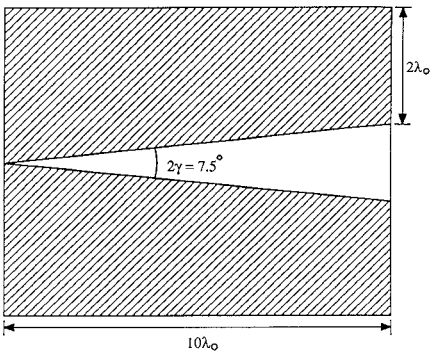

Fig. 5. Radiation patterns of an LTSA on Duroid 6010 substrate ($\epsilon_r = 10$). (a) Without cutting of substrate in tapered region. (b) With cutting the substrate in the tapered region. (c) Outline of the antenna.

E. Wide Opening Angle TSA's, Bandwidth Effects

The original Vivaldi antenna, as developed by Gibson [2], employed a taper which opened up much faster than the TSA's described so far in this paper. The effect of this is that the beam width, when plotted either versus frequency or normalized length, becomes constant instead of decreasing as predicted by the Zucker standard curves. Gibson measured a roughly constant beam width over a band of about two octaves. This effect can be qualitatively explained if one observes that the effective radiating length of the antenna at a given frequency is less than the total length, since the radiation tends to leave the antenna structure earlier, the shorter the wavelength is. Recently, DeFonzo and coworkers [13] have studied similar antennas in the time domain. For the TSA's with smaller opening angles, which are the main case discussed in the present paper, the beam width is of course dependent upon frequency, essentially as predicted by Zucker's curves. It also appears that a somewhat thicker substrate can be utilized for this type of TSA; for example, Gibson used a 0.25-mm-thick alumina substrate up to 40 GHz, an effective thickness according to (1) of about 0.07. Another class of TSA's (not covered here) has lengths of 1 to 2 wavelengths [14] and beam widths more similar to those of broadside integrated elements.

III. Characteristics of TSA Arrays

A. Beam Width, Directivity, and Gain of TSA Elements in Arrays

In most applications, the TSA array will be used as a focal plane array in conjunction with a reflector or lens focusing element (in order to be specific, we assume a

reflector antenna in what follows). We will therefore be interested in finding array parameters which result in equal *E*- and *H*-plane beam widths at about the −10 dB level in order to illuminate the reflector for maximum aperture efficiency. We will also be interested in the range of f/D values for the reflector for which it is feasible to design an efficient TSA array. It has been found that the most efficient TSA arrays are those with an element spacing of roughly 1–2 wavelengths. For element spacings larger than this, the radiation patterns become quite similar to those of single elements, as expected, so we will deal primarily with the arrays with the smaller spacings. Fig. 6 gives examples of how the −10 dB beam width varies with antenna element length, as measured at 35 GHz, for two LTSA arrays with the same element spacing of 1.5 wavelengths but different taper opening angle. As can be seen, fairly small changes in length may change the beam widths quite drastically. In both cases, one can find an antenna length for which the *E*-, *D*-, and *H*-plane beam widths are equal, however. A theoretical model which can predict the radiation patterns of TSA array elements has not yet been worked out, and one must find the optimum array parameters empirically. Efficient versions have been developed of both the LTSA and the CWSA type (see, for example, [15] and [16]).

While the directivity of single elements in principle may increase indefinitely with increasing antenna length, this is not possible for array elements, since the element gain is constrained by the area occupied in the array by each element. If we assume for simplicity an array with square symmetry, and with an element spacing of d, then the element area is d^2, and the element gain is limited to

$$G_{\max} = \frac{4\pi d^2}{\lambda^2}. \tag{3}$$

We have measured element gains for LTSA array elements by comparison with a standard gain horn and have found that they do indeed approach $G_{\max}$. As an example, Fig. 7 shows the measured gain from 27.5 to 40 GHz for a 5×5 element LTSA array with 1.5 λ_0 spacing at 35 GHz. $G_{\max}$ has also been plotted, and one can see that the average difference is about 0.5 dB. We can define $G/G_{\max}$ as the aperture efficiency for the array alone (note that this is different from the aperture efficiency for the reflector system, to be discussed in subsection III-B), and obtain about 90 percent for the above array (with a likely error of ±10 percent). The high aperture efficiency is unique to TSA arrays, and one should note that this efficiency is maintained over a waveguide band.

It is again interesting to compare the measured gain with the directivity estimated from the radiation patterns. If the directivity is derived in the standard manner from *E*- and *H*-plane patterns only, using (2), one obtains values which are typically about 2–3 dB higher than the measured gain, and considerably higher than $G_{\max}$ as well. This high directivity reflects the fact that the traveling-wave radiation mechanism successfully narrows the beam to a width which is unusually small for an element of the given

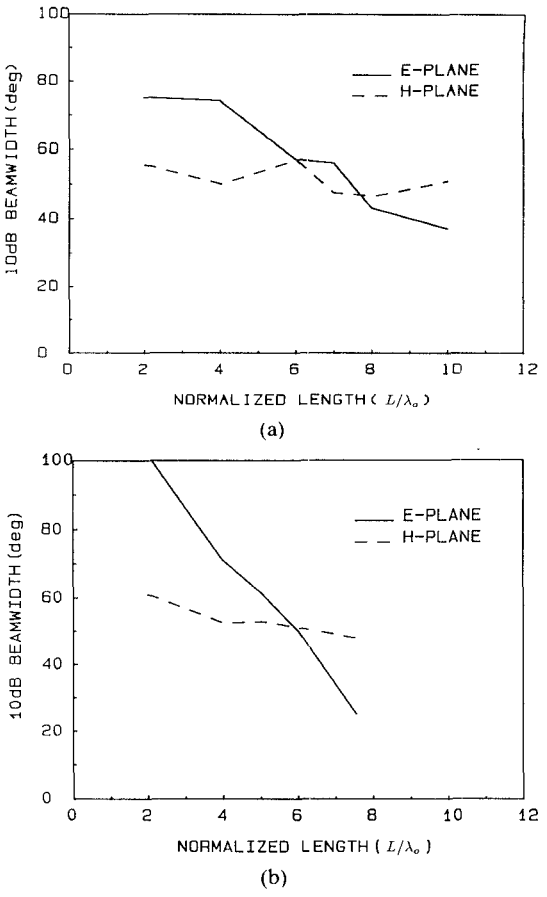

Fig. 6. 10 dB beam width versus normalized length for elements in a 5×5 LTSA array with $d/\lambda_0 = 1.5$ for (a) $2\gamma = 7.5°$ and (b) $2\gamma = 11.2°$.

size. If the directivity is instead obtained by integrating copolarized and cross-polarized patterns for the *E*, *H*, and *D* planes, as described for single elements, one typically finds a directivity which is about 1 dB higher than the measured gain. Since the measured gain must include ohmic and dielectric losses, these numbers are entirely consistent, within the measurement error. The integrated cross-polarized power radiated is typically about 20–30 percent of the total radiated power. One may also note that if a polarization filter, such as a grid, were to be placed in front of the array, the measured gain would be the same, while the cross-polarized lobes would be essentially eliminated. Typical radiation patterns for both polarizations in all three planes are given in Fig. 8.

B. Circuit Properties of TSA Array Elements

Elements in a typical broadside array, such as dipoles, with close element spacing, show substantial changes in the input impedance compared to isolated elements. TSA elements, however, show very little of these effects. Specifically, elements which are fed from a finline transition have a return loss at the waveguide ports of about 15 dB. Also, if one port is fed, the power coupled via the TSA array to the other waveguide ports is about 25 or 30 dB down. Shorting or open-circuiting other elements does not result in any detectable effects on the radiation pattern of a particular element. On the other hand, the forward coupling to neighboring radiating elements is often quite

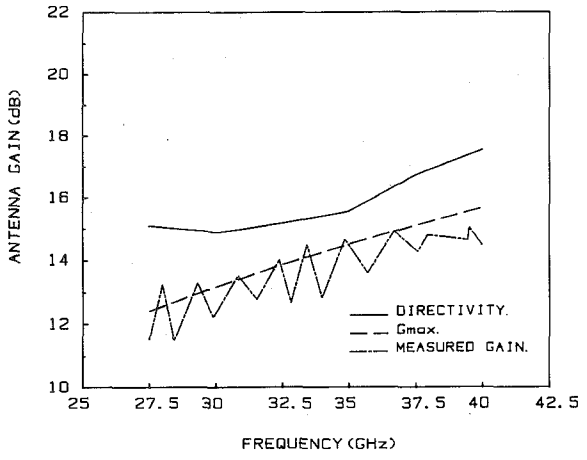

Fig. 7. Estimated directivity and measured gain versus frequency for an element in a 5×5 LTSA array. Parameters are $L/\lambda_0=7.6$, $d/\lambda_0=1.5$, and $2\gamma=11.2°$. G_{max} (see eq. (3)) has been plotted for comparison.

substantial, an effect which may be partly responsible for the high aperture efficiency of TSA arrays, which was discussed in the previous section.

IV. TSA Arrays as Focal Plane Arrays

One can also use the measured radiation patterns to estimate the aperture efficiency of a reflector antenna system which uses a TSA focal plane array. The best arrays developed so far achieve estimated system aperture efficiencies of 40–50 percent at element spacings of about 1–1.5 λ_0 for an $f/D=1$ system [15]. For f/D larger than about 1.5, the aperture efficiency decreases. It is important to note the small element spacing, since other types of elements yield wider beams, if compared at the same size as a TSA element, and consequently suffer spillover losses, which decrease the efficiency below that of TSA arrays [17]. The relative size of a CWSA array is compared in Fig. 9 with an array of conical horns which would yield the same element beam width.

V. Integration of TSA Elements with Circuits

TSA single elements and arrays lend themselves very well to integrating with different types of circuits. We have already shown how they can easily be fed from a waveguide, by using a finline transition section. It is also possible to directly let the tapered slot continue into a slotline circuit. In this case, one must note that the requirements placed on the dielectric are different for the TSA and the circuit portion of the substrate. The TSA prefers a thin dielectric with moderately low dielectric constant, while the slotline circuits are usually designed on substrates of dielectric constant of at least 10, and with a larger thickness. If implemented on a thin, low-dielectric-constant substrate, the slotline circuit may radiate too much, and show too large cross talk between different lines. This problem may be solved by making a transition to a transmission line such as coplanar waveguide, which would radiate less. Excellent transitions of this type are available, using MMIC technology [18], for example. An

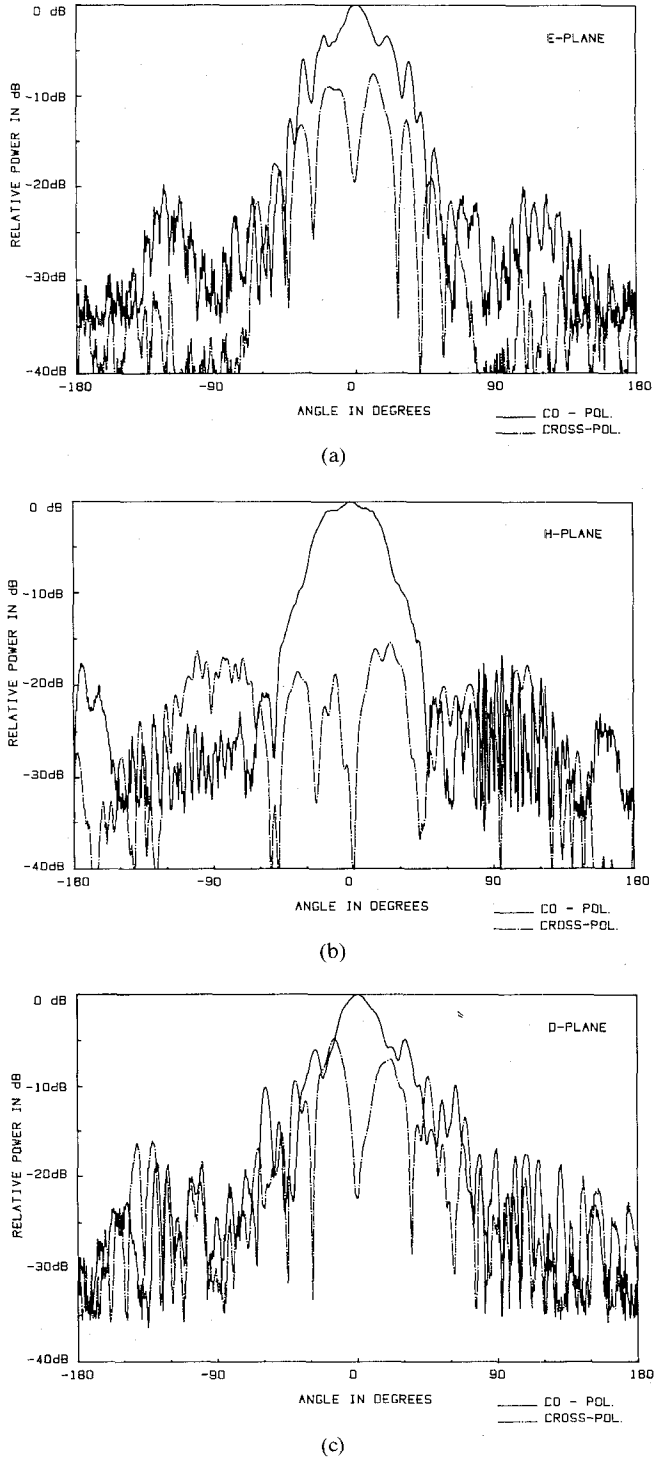

Fig. 8. Radiation patterns for an element in the array used for Fig. 7. (a) E Plane. (b) H Plane. (c) Diagonal (45°) plane.

alternative is to make use of the techniques for eliminating the substrate effects on the radiation pattern which were discussed in subsection II-D, in which case a semiconductor substrate of a convenient thickness may be employed. A further alternative is to use different substrates for the TSA and the circuit. In transmitting the signal between the two substrates, it is then also possible to make use of the coupling between the slotlines without necessarily having to make a direct electrical connection. In all cases where an open circuit configuration is used, one must be careful

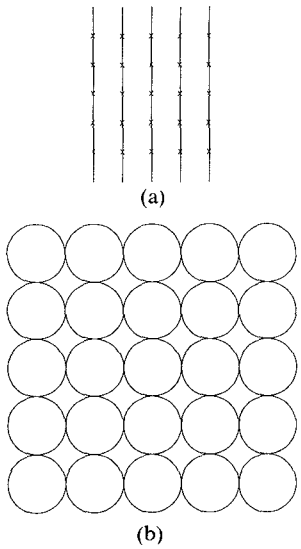

Fig. 9. Comparative size of arrays of (a) CWSA elements and (b) conical horn elements. Element patterns illuminate a reflector with −10 dB edge taper in both cases.

to design the circuit to minimize extraneous radiation, and some extra shielding may be required. In the following two sections, we will give some specific further examples of circuits which have been implemented.

VI. Applications of Single Elements

A. Broad-Band Detectors/Receivers

Gibson [2], in his pioneering paper, described Vivaldi single elements, with roughly constant −3 dB beam width of about 30–40° over a band of about two octaves. He was also able to match the Vivaldi element to a microstrip line over an even wider bandwidth: about 8–40 GHz.

B. Integrated SIS Mixer Receiver/CWSA

Two different SIS mixer receivers, integrated with CWSA single elements, are under development [19], [20]. The frequencies are 100 and 700 GHz, respectively. Both the signal to be received and the LO power are fed to the 100 GHz module (Fig. 10) from a lens waveguide system at the bottom of a liquid helium Dewar. The substrate used is quartz, which has been ground to 90 μm thickness in order to satisfy the maximum thickness criterion for the CWSA ($t_{\text{eff}}/\lambda_0 = 0.028$ according to (1)). A slot-to-microstrip transition is employed, and the mixer circuit is etched on the opposite side of the substrate. The series array of four lead indium/oxide/lead SIS junctions is connected in series with the microstrip at a point which is a virtual short circuit to ground. The IF frequency of 4 GHz is tapped off via a microstrip bandstop filter for the RF frequency. An interesting feature of SIS mixers is that the embedding impedance can be found by comparison of the measured and simulated $I-V$ characteristics. An initial test gave a DSB noise temperature of 250 K, but a considerable improvement is expected after the IF matching has been optimized. The radiation patterns of the CWSA were measured by using a diode instead of the SIS mixer; these are shown in Fig. 11.

The 700 GHz receiver [20] uses a CWSA etched on a silicon substrate (dielectric constant 11.6). Model experiments showed that good radiation patterns would be obtained if the silicon thickness could be etched to a thickness of 3–4 μm. Efforts are under way to investigate different processing procedures which will result in an antenna element with good radiation patterns. In this receiver, the Nb/Nb oxide/PbBi junctions are connected across the slotline, and the IF output occurs via a slotline filter. This integrated receiver/CWSA is expected to be tested in the near future. Both SIS receivers are being planned for eventual extension to focal plane arrays, to be used in imaging systems for millimeter-wave and submillimeter-wave radio astronomy.

C. Application of High-Gain Single-Element TSA's

Single-element TSA's could be employed when inexpensive moderate-gain antennas are required. As pointed out above, antenna gains up to 17 dB may be achieved, and low-cost receivers could be integrated with the TSA.

VII. Applications of Arrays

A. Multibeam Systems for Imaging

Arrays of feed elements placed in the focal plane of a reflector or lens can be utilized to sample the image produced by the optical system in that plane. According to the sampling theorem, the full information in a band-limited signal can be recovered if the signal is sampled at a rate which is twice the maximum frequency in the signal being sampled. Translated into terms appropriate for the imaging case, the frequencies in question are the spatial frequencies (dimension 1/length) into which the image may be decomposed, and application of a two-dimensional version of the sampling theorem shows that the feeds must be placed with an interval of (assuming that we are sampling incoherent radiation) [21]

$$T_I = \lambda_0/2 \times f - \# \tag{4}$$

where the $f-\#$ of the optical system is approximately equivalent to the f/D for the paraboloid case. In different terms, the sampling limit corresponds to a spacing between neighboring beams of 0.42 3 dB beam widths. Unfortunately, it can be shown that it is not possible to design an imaging system with this resolution which also has an aperture efficiency approaching that of typical single-beam systems [17]. Constructing feed arrays of metal waveguide horns, one finds that the feeds which yield high efficiency are so large that the element spacing is about four times the sampling-limited spacing, and the image will thus necessarily be undersampled. TSA arrays with spacings of 1–2 λ_0, as described above, can reach 40–60 percent aperture efficiency in typical systems, and sample the focal plane at about twice the sampling-limited spacing. This is an improvement in resolution by a factor of two (or a factor of four on an area basis), compared with typical array elements. The aperture efficiency of TSA arrays actually approaches the maximum aperture efficiency at this element spacing for an ideal element, which is about 60 percent [17]. For twice this spacing the maximum

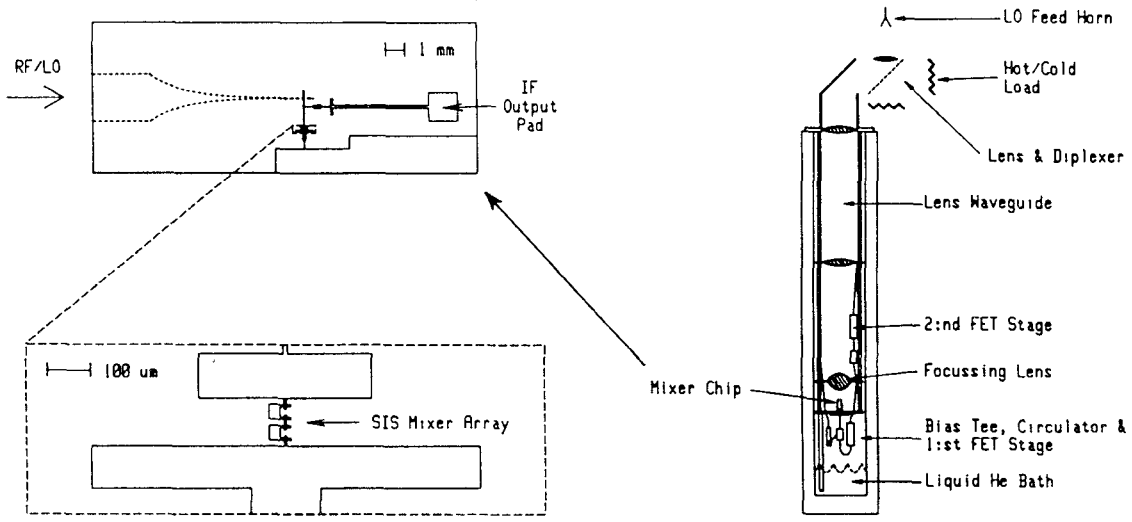

Fig. 10. Schematic diagram of 100 GHz SIS mixer/CWSA receiver system. Details are shown for the mixer "chip."

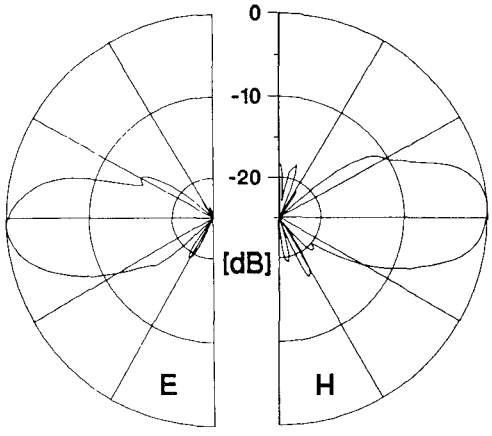

Fig. 11. Radiation patterns of the CWSA used for the receiver in Fig. 10.

aperture efficiency is 80 percent. In order to determine the relative overall advantage which will be realized when using different types of arrays, a detailed analysis of all these factors is required, taking into account the desired requirements of the specific system. Also considering the advantage of ease of construction, TSA arrays appear attractive for millimeter-wave imaging systems applied in radio astronomy, remote sensing, or surveillance.

Prototype systems have been built which have verified the optical performance of reflector antennas with simple focal plane TSA arrays. The first such system [22] utilized a seven-element array with a hexagonal arrangement of the elements in a Cassegrain telescope with a 30-cm-diameter main reflector. The frequency was 94 GHz, and the TSA's were fabricated on 25 μm Kapton substrates. Test signals from a source in the far-field region were detected directly by diodes soldered across the narrowest portion of the tapered slot. A minimum beam spacing of 0.5° was measured, when the elements were 1.6 λ_0 apart. This represents a little less than twice the sampling limit spacing. Fig. 12 shows this system. The Cassegrain telescope was also used with a four-element array for demonstrating tracking, by using the detected signals in an incoherent monopulse mode. Extensions to coherent monopulse applications appear feasible. One should also note that the sampling-limited spacing for *coherent radiation* is twice the value given by (4). Thus, future coherent imaging systems may reach the sampling-limited resolution.

In another application to imaging systems, a 5×5 element CWSA array was used at 31 GHz to demonstrate the optical performance in a prime-focus paraboloid with a 30 cm diameter [16]. Fig. 13 shows the beams recorded from the five elements on one of the substrates of this array. The system was also successfully used to resolve a double point source (two conical horns), with an angular separation given by the Rayleigh criterion used to characterize optical instruments [23].

B. Multibeam Satellite Communication Systems

Multibeam satellite communication antennas also employ feed arrays. Integrated arrays would have a significant weight advantage in such systems if they could be designed with efficiencies similar to those of presently used waveguide arrays. The considerations regarding aperture efficiency versus element spacing which were reviewed in subsection A would apply in this case as well. The parameter most often discussed in this application is the crossover level between neighboring beams. For example, TSA array elements can be stacked so that the spacing corresponds to one 3 dB beam width, yielding a crossover level of −3 dB. This crossover level is considerably higher than would be obtained with conventional arrays, and would make it worthwhile to consider TSA arrays for beam-shaping and beam-switching applications.

C. Power Combining

Power combining of many sources offers a method of making higher output powers available when the amount of power from a single source is low, as is the case for most solid-state sources. The high aperture efficiency of the array proper (greater than 80 percent, see subsection III-A) and the small element spacing make TSA arrays attractive for this application. A linear four-element LTSA array has been used for inter-injection-locked power combining by

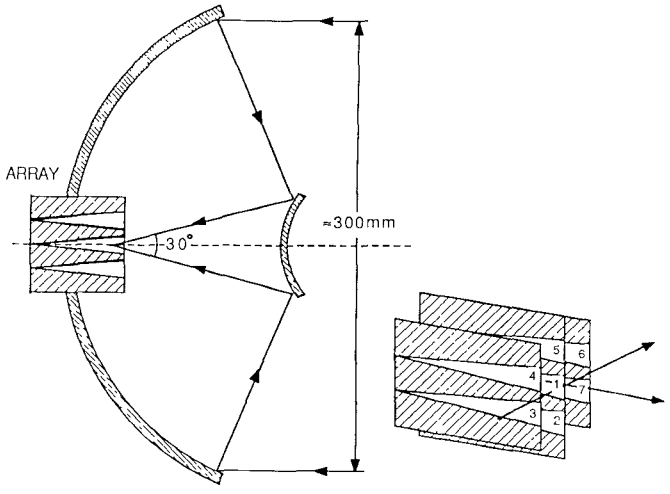

Fig. 12. Schematic diagram of 94 GHz Cassegrain seven-element imaging system.

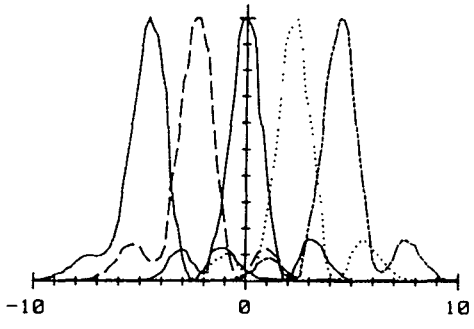

Fig. 13. Radiation patterns for five elements in a 5×5 CWSA imaging array for 31 GHz. (Linear power scale.)

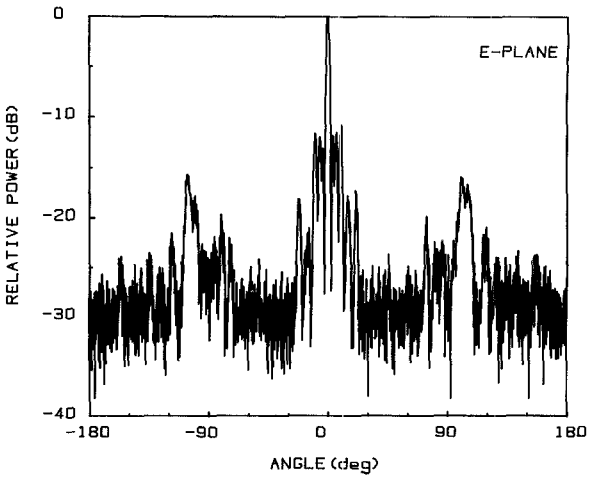

(a)

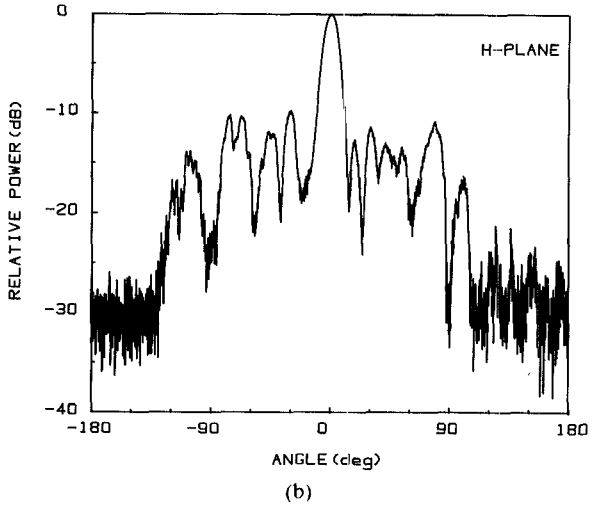

(b)

Fig. 14. Radiation patterns at 35 GHz of a 32-element linear phased array of LTSA elements. (a) *E* plane. (b) *H* plane.

Morgan and Stephan [24]. In another typical configuration, the power from a number of (MMIC type, for example) power amplifier modules may be combined phase coherently in a TSA array, and the array used to feed a near-field Cassegrain antenna, as previously demonstrated with cigar antenna elements [25]. The small spacing of the TSA elements would translate into a higher packing density, and a higher total power radiated in this case, since the total array size would be limited by the size of the subreflector. The small coupling between the circuit ports of the TSA elements would also be an advantage.

D. Phased Arrays

Typical phased arrays are designed for wide-angle scanning and require short elements with wide element patterns. The "notch antenna" [26] is an element, similar to the TSA, which is used for such arrays. The longer, narrower beam elements which we review in this paper could also be used in phased arrays when the requirements call for scanning over smaller angles. We have measured the radiation patterns in the *E* and the *H* plane of a linear 32-element array of LTSA elements, with a spacing of about 0.66 λ_0, as shown in Fig. 14. A slotline feed network was used. Grating lobes are decreased in amplitude due to the narrow element pattern, as expected. Integrated TSA phased arrays thus could be attractive as low-cost alternatives to other presently used arrays.

VIII. Conclusion

TSA's have characteristics which are presently well understood in their main features, both as single elements and as arrays. This paper has pointed to a number of application areas and has given information with which TSA's can be evaluated for potential use in these areas. Much still remains to be learned about TSA's, however, especially about the cross-polarized radiation and the complicated mutual coupling effects which make TSA arrays work efficiently.

Acknowledgment

The authors gratefully acknowledge cooperation and discussions with a number of colleagues and the encouragement from M. C. Bailey and B. Kendall at NASA LaRC.

References

[1] R. J. Mailloux, "Phased array architecture for millimeter wave active arrays," *IEEE Antennas Propagat. Soc. Newsletter*, Vol. 28, p. 3, Feb. 1986.

[2] P. J. Gibson, "The Vivaldi aerial," in *Proc. 9th European Microwave Conf.* (Brighton, U.K.), 1979, pp. 101–105.

[3] C. Yao, S. E. Schwarz, and B. J. Blumenstock, "Monolithic integration of a dielectric millimeter-wave antenna and mixer diode: An

embryonic millimeter-wave IC," *IEEE Trans. Microwave Theory Tech.*, vol. MTT-30, p. 1241, 1982.
[4] H. Jasik, Ed., *Antenna Engineering Handbook*. New York: McGraw-Hill, 1961, p. 16–14.
[5] R. Janaswamy, D. H. Schaubert, and D. M. Pozar, "Analysis of the transverse electromagnetic mode linearly tapered slot antenna," *Radio Sci.*, vol. 21, pp. 797–804, 1986.
[6] K. S. Yngvesson *et al.*, "Endfire tapered slot antennas on dielectric substrates," *IEEE Trans. Antennas Propagat.*, vol. AP-33, pp. 1392–1400, 1985.
[7] T. Thungren, E. L. Kollberg, and K. S. Yngvesson, "Vivaldi antennas for single beam integrated receivers," presented at *12th European Microwave Conf.* Helsinki, Finland, 1982.
[8] R. Janaswamy and D. H. Schaubert, "Analysis of the tapered slot antenna," *IEEE Trans. Antennas Propagat.*, vol. AP-35, pp. 1058–1065, 1987.
[9] J. Johansson, in preparation.
[10] T. K. Korzeniowski, "A 94 GHz imaging array using slot line radiators," Ph.D. thesis, University of Massachusetts, Sept. 1985.
[11] R. Janaswamy, "Radiation pattern analysis of the tapered slot antenna," Ph.D. thesis, University of Massachusetts, Aug. 1986.
[12] R. Carrel, "The characteristic impedance of two infinite cones of arbitrary cross-section," *IRE Trans. Antennas Propagat.*, pp. 197–201, 1958.
[13] A. P. DeFonzo and C. R. Lutz, "Optoelectric transmission and reception of ultrashort electrical pulses," *Appl. Phys. Lett.*, vol. 51, pp. 212–214, July 1987.
[14] S. N. Prasad and S. Mahapatra, in *Proc. 9th European Microwave Conf.* (Brighton), 1979, pp. 120–124.
[15] Y. S. Kim and K. S. Yngvesson, "Aperture efficiency of LTSA focal plane arrays for millimeter waves," in *Proc. 12th Int. Conf. Infrared and Millimeter Waves* (Lake Buena Vista, FL) Dec. 1987, pp. 220–221.
[16] K. S. Yngvesson, J. F. Johansson, and E. L. Kollberg, "A new integrated feed array for multi-beam systems," *IEEE Trans. Antennas Propagat.*, vol. AP-34, pp. 1372–1376, 1986.
[17] K. S. Yngvesson, J. F. Johansson, Y. Rahmat-Samii, and Y. S. Kim, "Realizable feed-element patterns and optimum aperture efficiency in multi-beam antenna systems," *IEEE Trans. Antennas Propagat.*, Nov. 1988.
[18] T. Hirota, Y. Tarusawa and H. Ogawa, "Uniplanar MMIC hybrids —A proposed new MMIC structure," *IEEE Trans. Microwave Theory Tech.*, vol. MTT-35, pp. 576–581, 1987.
[19] A. Skalare, J. Johansson, E. Kollberg, and R. Murowinski, "Integrated slot-line antennas with SIS mixers for focal plane applications," *17th European Microwave Conf.* (Rome), Sept. 1987, pp. 461–465.
[20] D. Winkler *et al.*, "A new submillimeter wave SIS quasi-particle receiver for 750 GHz," in *Proc. 11th Int. Conf. Infrared Millimeter Waves* (Pisa, Italy), Oct. 1986.
[21] J. W. Goodman, *Introduction to Fourier Optics*. New York: McGraw-Hill, 1968.
[22] T. L. Korzeniowski, D. M. Pozar, D. H. Schaubert, and K. S. Yngvesson, "Imaging system at 94 GHz using tapered slot antenna elements," presented at *8th Int. Conf. Infrared Millimeter Waves*, 1983.
[23] M. Born, and E. Wolf, *Principles of Optics*. Pergamon, Oxford (1980).
[24] W. A. Morgan and K. D. Stephan, "Inter-injection locking—A novel phase-control technique for monolithic phased arrays," in *Proc. 12th Int. Conf. Infrared Millimeter Waves* (Lake Buena Vista, FL), Dec. 1987, pp. 81–82.
[25] K. Woo *et al.*, "*X*-band high-gain antenna with solid-state transmitter," in *Int. AP Symp. Dig.* (Seattle, WA), June 1979, pp. 465–468.
[26] L. R. Lewis, M. Fasset, and J. Hunt, "A broadband stripline array element," in *IEEE AP-S Symp.*, June 1974, p. 335.

✠

K. Sigfrid Yngvesson (M'62) received the degrees of Civilingenjor (B.S.), tekn. Lic. (M.S.), and Tekn. Dr. (Ph.D.) in 1958, 1965, and 1968, respectively, from the Electrical Engineering Department of Chalmers University of Technology, Gothenburg, Sweden, majoring in electron physics. He has worked on masters and millimeter-wave receivers for radio astronomy, including a 60-GHz system for the Space Shuttle. He is also active in developing imaging antennas and integrated millimeter-wave receivers. He is currently a Professor in the Department of Electrical and Computer Engineering of the University of Massachussetts in Amherst.

✠

T. L. Korzeniowski (S'82–M'83), photograph and biography not available at the time of publication.

✠

Young-Sik Kim received the M.Sc. degree in electrical engineering from Korea University in September 1977. He has been a research assistant in the Department of Electrical and Computer Engineering at the University of Massachusetts, Amherst, where he received the Ph.D. degree in June 1988. He is presently a Post-doctoral Scholar at the University of Massachusetts. Dr. Kim has worked on ferroelectric phase shifters as well as TSA single elements and focal plane arrays for millimeter waves.

✠

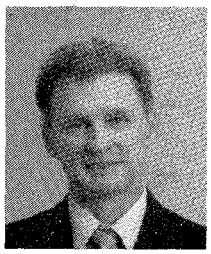

Erik L. Kollberg (M'83–SM'83) received the M.Sc. degree in 1961 and the Teknologie Dr. degree in 1971 from Chalmers University of Technology, Göteborg, Sweden.

He has been a Professor at the same university since 1974. Dr. Kollberg has published more than one hundred scientific papers in international journals in the field of maser amplifiers, millimeter-wave Schottky diode mixers, superconducting mixers, GaAs devices, and other subjects related to millimeter-wave techniques. He is responsible for the development of low-noise receivers for the Onsala Space Observatory and the new Swedish–European millimeter-wave telescope in Chile.

Dr. Kollberg received the microwave prize at the European Microwave Conference in Helsinki 1984 and is the chairman of the Swedish IEEE MTT-S Chapter.

✠

Joakim F. Johansson was born in Töllsjö, Sweden, on November 3, 1959. He received the degrees of Civilingenjör (M.Sc.) in electrical engineering and the Teknologie Licentiat in radio and space science, both from Chalmers University of Technology, Gothenburg, Sweden, in 1983 and 1986, respectively. He received the Ph.D. degree in September 1988. He spent seven months as a visiting scholar with the Department of Electrical and Computer Engineering University of Massachusetts, Amherst, during 1986/87. His research interests include imaging using arrays of tapered slot antennas, quasi-optics for mm and sub-mm receiver systems, and numerical electromagnetics.